

Evaluation of Heterogeneity Impact on Hydraulic Fracturing Performance

Hadi Parvizi^a, Sina Rezaei-Gomari^{a*}, Farhad Nabhani^a, Andrea Turner^b

^a School of Science and Engineering, Teesside University, Middlesbrough, TS1 3BA, UK

^b EON E&P, 129 Wilton Road, London, SW1V 1JZ, UK

Abstract

Hydraulic fracturing operation in tight reservoirs increases the connectivity of the well to more reservoir layers and further regions, thus boosting the production. Heterogeneity influences the hydraulic fracturing performance; this is observed when comparing the performance of different fraced wells. Those that far outperform other fraced wells are generally connected to more permeable rock or natural fractures.

Modelling hydraulic fracturing net pressure provides hydraulic fracture dimensions and connectivity per fracture job. Moreover, well test interpretation can imply the active number of hydraulic fractures and an average estimation of their dimensions and connectivity after cleaning up and flowing the well. There is a technical gap in the integration of well test data with fracing operational data for diagnosing and evaluating the hydraulic fracture performance. This paper introduces a novel approach to link the hydraulic fracturing modelling with well test interpretation. This method quantifies heterogeneity impact on hydraulic fracture performance through introducing a new parameter defined as Heterogeneity Impact Factor (HIF). The calculated HIF for the fraced wells varies between 74 % (indicating that the well far outperformed the expected hydraulic fracture performance) to -65 % (dramatically underperformed well). The outcome of the proposed technique was validated by geological observations and was subsequently applied to the dynamic simulation model. The pressure prediction of the model was compared with the three-week annual shut-down; the build-up response

* Corresponding author. Tel.: +44 7847012063
E-mail address: s.rezaei-gomari@tees.ac.uk (Sina R. Gomari).

24 and its derivative display an excellent match which provides evidence for the robustness of the
25 dynamic model and the effectiveness of the proposed technique.

26 **1. Introduction**

27 Since its introduction in the late 1940s, hydraulic fracturing has been widely used in North America to
28 achieve higher recovery from low permeability reservoirs and/or to bypass the formation damage
29 around the wellbore (Economides, et al., 2002). In addition, successful applications of this technique
30 have been reported in other locations including North Sea (Vos, et al., 2009), South America (Antoci
31 and Anaya, 2001), Asia (Shaoul, et al., 2007) and Middle East (Al-Zarouni and Ghedan, 2012) and
32 (Mirzaei-Paiaman, 2013). Generally, many steps of analysis are performed prior to any hydraulic
33 fracturing job to ensure its effectiveness. But, in comparison, hydraulic fracturing in heterogeneous
34 reservoirs requires much more analysis for an optimum design and operation. This is mainly due to
35 the fact that in heterogeneous reservoirs, rock properties vary dramatically and can affect the hydraulic
36 fracture performance. To overcome the technical and operational challenges associated with hydraulic
37 fracturing in such reservoirs, multi-disciplinary approaches are required to gain improved insight into
38 the hydraulic fracturing performance. This aim can be fulfilled by developing methods to capture the
39 impacts of reservoir heterogeneity, most desirably in a quantitative manner, in a way that the results
40 can be easily translated into reservoir dynamic modelling systems.

41 Southern North Sea (SNS) reservoirs are among the most heterogeneous reservoirs in which hydraulic
42 fracturing has been considered for implementation. The SNS reservoirs are characterised by their more
43 permeable layers and natural fractures as the two possible elements of heterogeneity (Parvizi, et al,
44 2015a) and (Parvizi, et al, 2015b). These distinctions make the fraccing designs more complicated and
45 signify the importance of taking an integrated approach to get the most out of the available data.
46 However, integration of different data sources is often not straightforward and requires innovative
47 techniques. This paper introduces a new technique to diagnose the hydraulic fracture performance by

48 integrating well test analysis and collecting data at each hydraulic fracturing stage. Upon identification
49 of a technical gap in data integration, this paper proposes an innovative technique for quantifying the
50 impact of heterogeneity on hydraulic fracture performance. Results observed after applying this
51 technique to real field data provide robustness to the method.

52 There are different approaches to evaluate the well performance of a hydraulically fractured well. Each
53 approach has its own advantages and requires a different level of details for modelling. Accordingly,
54 the prediction reliability depends on the methodology strength in capturing more of the contributing
55 production mechanisms and the underlying physics.

56 The most common modelling approaches for incorporating the effects of hydraulic fracturing include
57 negative well skin factor (Schulte, 1986), course-grid transmissibility multiplier (El-Ahmady and
58 Wattenbarger, 2004; Iwere et al., 2004), and local grid refinement (LGR) transmissibility modification
59 (Bennett, et al., 1986; Hegre, 1996). The LGR method offers more modelling flexibility since 3D
60 properties with higher resolution can be modelled to help incorporate the reservoir heterogeneity.
61 Ideally, the fracture cell (i.e. the cell which hosts the induced fracture) should have similar width to
62 the induced fracture which can be, for example, in the range of 0.03 to 0.51 inches (based on the data
63 from 24 hydraulic fracture jobs performed in a Southern North Sea field; see Appendix A). Using such
64 small cell sizes violates one of the assumptions of well modelling in finite difference simulators
65 (Peaceman radius formula) and adds error to the well performance calculations. It is also extremely
66 slow and generates convergence problems in numerical reservoir simulations (Hegre, 1996). One
67 solution is to consider thicker fracture cells and upscale the hydraulic fracture conductivity to the
68 fracture cells.

69 In the presence of natural fractures in tight formations, the physics and modelling become more
70 complicated and challenging. Due to difficulties of designing and performing experimental work on
71 fracture network propagation in the laboratory settings and the difference of laboratory and reservoir
72 scales, numerical modelling has become an essential tool in hydraulic fracture studies, as it facilitates

73 incorporation of many details and conditions in modelling and prediction of fracture network
74 geometries (Zhang et al., 2015). Some authors have attempted to simulate hydraulic fracturing in
75 naturally fractured reservoirs considering the complexities involved. Fracture modelling approaches
76 based on the Boundary Element System (BES) were applied by some researchers (Sousa et al., 1993;
77 Zhang et al., 2007; Sesseetty and Ghassemi, 2012). Zhao and Young (2009) developed a dynamic 3D
78 Distinct Element Model (DEM) based on tri-axial fracturing laboratory experiments to simulate fluid
79 injection into a reservoir with natural fractures. Ben et al. (2012) used Discontinuous Deformation
80 Analysis (DDA) to simulate hydraulic fracturing. Huang and Ghassemi (2012) used the Virtual
81 Multidimensional Internal Bonds (VMIB) evolution function for numerical simulation of 3D fracture
82 propagation at micro scale. Using this method, they successfully represented the features of tensile and
83 compressive fracture propagation and suggested that 3D simulation of fracture propagation helps
84 understanding and designing multiple hydraulic fractures. Zhang et al. (2016) used the lattice cell
85 version of the discretized virtual internal bond method to model the reservoir rock for numerical
86 simulation of the fracture development behaviour in complex unconventional reservoirs.

87 Hamidi and Mortazavi (2014) simulated the hydraulic fracture initiation and propagation through
88 intact rock using 3D Distinct Element Code (3DEC) and introducing a fictitious joint technique to
89 facilitate importing the fracture initiation capability in the DEM approach. Zhang et al. (2015) have
90 given a full account of hydraulic fracturing simulation approaches and concluded that Displacement
91 Discontinuity Models (DDM) can best simulate the complex fracture networks.

92 Considering the fact that most of the numerical fracture modelling approaches are mainly suitable for
93 hard rocks due to assuming planar fracture geometry and linear plastic fracture mechanics, Wang
94 (2015) used Extended Finite Element Method (XFEM) together with Cohesive Zone Method (CZM)
95 and Mohr-Coulomb theory of plasticity to investigate the initiation and development of non-planar
96 fractures in brittle and ductile rocks. To address the same issues and investigate non-planar hydraulic
97 fractures by 3D simulation, Sobhaniaragh et al. (2016) also combined the Cohesive segments with

98 Phantom Node Method and called it CPNM. Nadimi et al. (2016) presented a new meshfree 3D
99 simulation model based on Peridynamic (PD) method for investigation of hydraulic fracture
100 development and geometry in complex and heterogenous formations; the method also considers the
101 interaction of the induced fractures with the natural fractures.

102 Despite their basic nature, coupling of these models with a commercial simulator for investigating the
103 interaction of induced fractures with natural fractures is difficult and currently not fully practical.

104 Therefore, on performance evaluation of hydraulic fractures, a methodology is required that can:

- 105 1. Serve as diagnostic tool to identify the heterogeneity in terms of natural fractures and/or high
106 permeability streaks;
- 107 2. Support the tuned initial guess for connectivity calculation of upscaled fracture cells to
108 reduce the associated uncertainty;
- 109 3. Link the findings to geological features.

110 These features have not been quantitatively integrated in the methodologies proposed by the
111 investigators so far. In this work, the authors suggest that such a technical gap can be filled through
112 integration of well test results with fracturing operational data analysis for diagnosing and evaluating
113 hydraulic fracturing performance. To link the hydraulic fracturing modelling with well test
114 interpretation, in this paper, a new methodology is proposed to quantify the heterogeneity impact on
115 hydraulic fracture performance in terms of a new parameter defined as Heterogeneity Impact Factor
116 (HIF). This parameter represents a quantified value for the expected performance of hydraulic
117 fracturing on each well considering the contribution of heterogeneity. HIF creates a basis for
118 comparing the wells of the same field with each other and also can exhibit the degree of heterogeneity
119 in different fields.

120 Quantification of heterogeneity impact as a value is important as it can be used for prediction of well
121 production by integrating the tools of production simulation with HIF. The way forward is to work on
122 a new methodology of integrating HIF with Decline Curve Analysis.

123 The results of the application of the proposed technique in one of the SNS reservoirs were in very good
124 agreement with geological and drilling observations. The HIF analysis was then incorporated into the
125 dynamic simulation model and pressure predictions of the model were compared with the three-week
126 annual shut-down. The build-up response and its derivative displayed an excellent match which
127 provides evidence of successful application of the proposed technique.

128 In the following sections, first, the workflow introduced by the authors in a previous study (Parvizi, et
129 al, 2015b) to analyse the hydraulic fracture performance is discussed. In that study, an integrated multi-
130 disciplinary approach was proposed for deploying the data and information available all the way from
131 seismic interpretation to reservoir dynamic modelling to evaluate the performance of the hydraulic
132 fracturing. It should be noted that the current work is, in fact, a continuation of the previous study and
133 the newly proposed HIF analysis is built upon the foundation of the hydraulic fracture performance
134 analysis workflow. For this reason, an in-depth discussion on the application of this workflow for the
135 reservoir under the study has been presented as well. Then, a new ratio (WTA/NPM) for evaluating
136 the performance of fraced wells as well as a new parameter (HIF) to show the impact of reservoir
137 heterogeneity have been defined and applied to the real field data. It is worth mentioning that the
138 methodology in this study is, indeed, focused on combining the results of well test analysis (where the
139 production-pressure is matched) with the results of net-pressure match (where pressure depletion is
140 characterized and matched using specific parameters). Once these two matches are obtained, since well
141 test considers a larger radius of investigation and net-pressure considers a smaller radius of
142 investigation, the relation between them can be used to conclude a zero-dimension property of the
143 reservoir heterogeneity which we have quantified and defined as HIF. Finally, the results of the work

144 are compared with geological evidences and validated by matching the pressure predictions of the
145 resulting dynamic reservoir model with the real well test data.

146 **2. Methodology: Hydraulic Fracture Performance Analysis Workflow**

147 In this section, the details of application of the comprehensive workflow of hydraulic fracture
148 performance analysis introduced by the authors in a previous publication (Parvizi, et al, 2015b) is
149 presented. In this work, actual field data was acquired from an oil and gas operator with the view to
150 evaluate the hydraulic fracture performance.

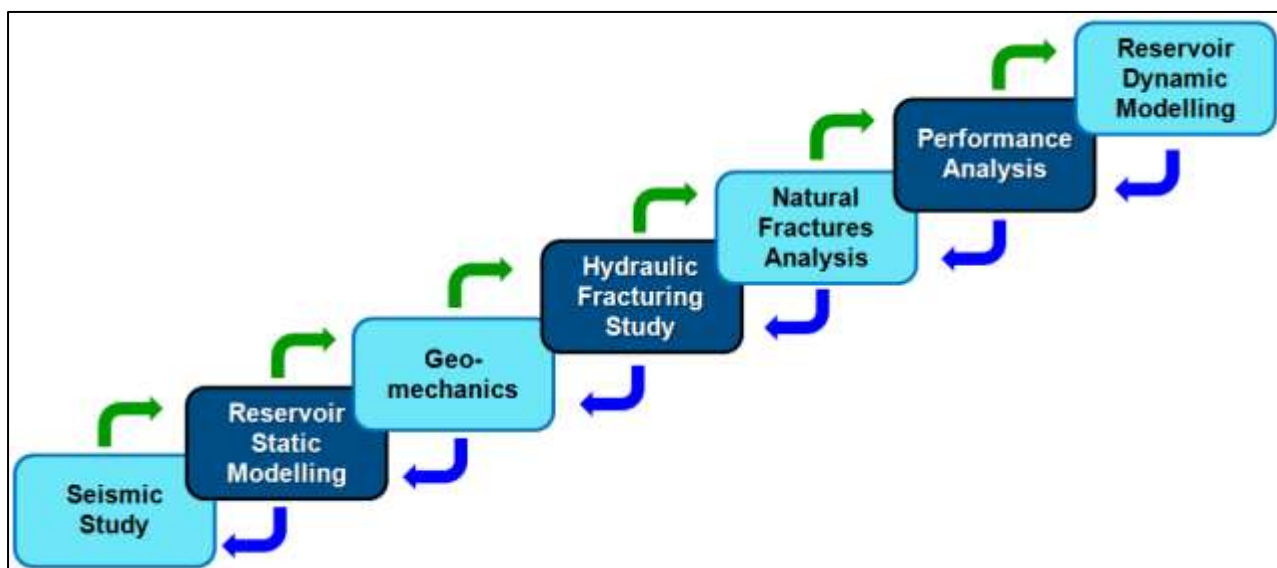
151 This field is situated in the Southern North Sea gas basin. It is 10 km long, 1.5 km wide with an
152 estimated reservoir thickness of 270 ft. The reservoir rock is of Rotliegend age, mainly sandstone with
153 layers of siltstone and minor shale deposits, according to log and core data. This producing horizon is
154 overlain by a 400-foot shale formation which constrains the propagation of the fractures. The reservoir
155 formation is also underlain by a very tight sandstone with unsuccessful attempts of production which
156 render it unexpected to have noticeable contribution to production of fluids. Based on core data, the
157 reservoir porosity ranges from 5 to 20 percent and the average reservoir permeability is less than 1
158 mD. Slightly higher permeabilities are observed where the reservoir formation is encountered in wells
159 at lower depths with less illitisation.

160 The initial well test, done on the exploration well in the 1980's, had indicated a gas flow rate of 4
161 MMSCFD; the low rate was attributed to the significantly illitised formation. An appraisal well was
162 drilled 16 years later and flowed 10 MMSCFD. A phased development plan was prepared with three
163 of the five initially planned horizontal wells (A, B, and C) being drilled and fraced each with five
164 stages. The two remaining wells were drilled after three years of production. These wells were also
165 horizontal each with five stage frac zones (D and E), similar to phase-1 wells.

166 Performance evaluation of these multi-fraced horizontal wells is crucial for forecasting and evaluating
167 further development opportunities. To simulate the hydraulic fracture in this study, pseudo 3D

168 hydraulic fracture modelling was performed using a commercial simulator for fracture design and
169 analysis in complex situations. However, it should be noted that, in this paper, the focus is on the
170 combined use of hydraulic fracture modelling results and pressure decline analysis results regardless
171 of the specific methodologies/ software used for obtaining such results. In other words, in any other
172 similar study, once the fracture modelling is performed using any approach chosen by the engineer/
173 researcher, the results can be integrated with the results of well test analysis, which could, in turn, be
174 accomplished using any method selected. Such integration of the results is then governed by the
175 workflow presented here.

176 A complete picture of the hydraulic fracturing modelling workflow requires an integrated multi-
177 disciplinary approach to be applied. This systematic workflow is shown in Figure 1 based on an ideal
178 approach of deploying multi-disciplinary information.



179

180 Figure 1. Integrated hydraulic fracturing modelling workflow proposed by Parvizi et al. (2015b).

181 The workflow ends in creating 3D static and dynamic models. Some of the fundamental inputs to the
182 workflow of hydraulic fracture performance evaluation are:

183

1. Results of net pressure match

184

2. Well test interpretations (pressure transient analysis)

- 185 3. PLT outcomes (production-data analyses)
- 186 4. Hydraulic fracture conductivity versus effective stress

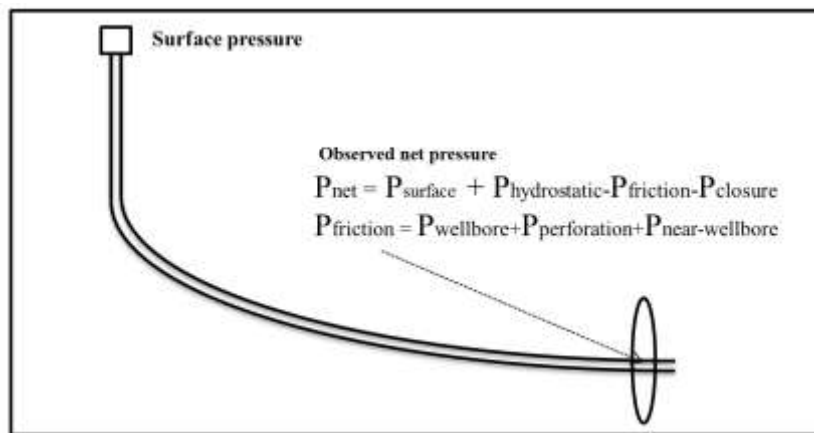
187 The details of each input as well as their integration in the fracture modelling are as follows:

188 **2.1 Net Pressure Analysis**

189 The difference between the pressure in the fracture and the in-situ stress (P_f – in-situ stress) is referred
 190 to as the net pressure. To estimate the patterns of growth for fractures in the field or after the treatment,
 191 the behaviour of net-pressure was defined by Nolte and Smith (1981). In their analysis method, they
 192 used the model proposed by by Perkins and Kern (1961) and later modified by Nordgren (1972) and
 193 hence called Perkins-Kern-Nordgren (PKN) theory. Based on the assumptions of the PKN theory, as
 194 long as the fracture height is contained, the net pressure will increase with time according to the
 195 following proportionality:

196 $P_n \propto \Delta t^e$

197 Where P_n is critical net pressure and Δt is change in time with $0.125 < e < 0.20$, and, slope, $e = 0.20$ for
 198 low leakoff and 0.125 for high leakoff. Leak off is a measure of the fracture fluid-loss when the
 199 pumping stops (Economides and Nolte, 2000).



200
 201 Figure 2. Net pressure calculation diagram.

202 Figure 2 is generated based on net pressure formulas Nolte and Smith (1981) defined. This Figure

203 shows the relationship between net pressure and the rest of measurements during fracturing operation.
204 Fracture geometry is inferred from net pressure and leak-off behaviour in this indirect diagnostic
205 technique. The results of net-pressure match interpretations are non-unique so careful application is
206 required. This technique is most useful when results are integrated or calibrated with results of other
207 diagnostics.

208 In a hydraulic fracturing job, the injection parameters (i.e. surface pressure, bottomhole pressure, flow
209 rate, fluid volumes, and proppant concentration) are recorded in real-time and fed into hydraulic
210 fracture modelling software. The software utilizes the closure stress profile and rock mechanical
211 properties from the static model to match the net pressure obtained from the injection parameters and
212 leak-off behaviour.

213 Through net pressure matching, an estimate of the fracture half-length x_f , fracture height h_f , fracture
214 width w_f and its conductivity C_{fD} was achieved for the number of fracture jobs implemented in this
215 field (Table 1).

216 **2.2 Well Test (Pressure Transient) Analysis**

217 It is possible to estimate of the number of active hydraulic fractures, their average fracture geometry
218 (fracture height and half-length) and their average conductivity using well test analysis. Clarkson
219 (2013) described very detailed and comprehensive approach of production data analysis including well
220 test interpretation for unconventional resources. There are three analytical well test models describing
221 fluid flow and pressure behaviour of hydraulic fractures:

- 222 • Infinite conductivity hydraulic fractures
- 223 • Uniform flux hydraulic fractures
- 224 • Finite conductivity hydraulic fractures

225 In infinite conductivity hydraulic fractures, it is assumed that pressure drop along the fracture is
226 negligible; therefore, fracture linear or bilinear flows are not practically observed. On a logarithmic
227 plot, the formation linear flow is seen with a slope of 0.5 followed by a pseudo-radial flow for which
228 the derivative becomes horizontal.

229 Flow in uniform flux hydraulic fractures behaves very similarly to infinite conductivity fracture, except
230 that the flow is assumed uniform along the fracture length. Formation linear flow and pseudo-radial
231 flow regimes can be observed if flow duration is long enough.

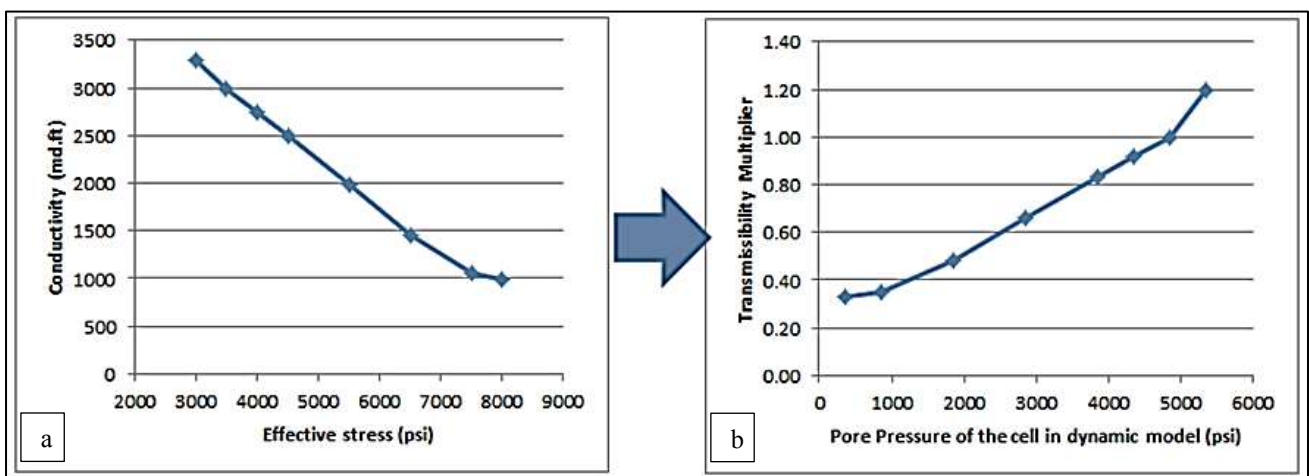
232 There is a considerable pressure drop along the finite conductivity hydraulic fractures, therefore
233 bilinear flow (fracture linear flow and formation linear flow) occurs at early times. Bilinear flow is
234 observed with the slope of 0.25 on the pressure derivate plot. Then linear formation flow may or may
235 not be seen, because it is very short and finally, pseudo-radial pressure behaviour is developed. During
236 the well test matching process of the five multi-staged fractured horizontal wells, finite conductivity
237 hydraulic fractures was assumed. This is because of uniform flux and infinite conductivity fracture
238 assumption lead to a different pattern of pressure behaviour comparing with the real data.

239 **2.3 Production Data Analysis**

240 Productivity of each fracture may be obtained from PLT analysis and deployed to validate the expected
241 flow contribution from net-pressure analysis, to check the number of active fractures obtained from
242 well test interpretation and to tune the dynamic model. It is commonly believed that a hydraulic
243 fracture with higher proppant concentration should perform better however, due to heterogeneity it
244 may be difficult to find a correlation between hydraulic fracture geometry, its proppant coverage and
245 production performance. Therefore, PLT has a key role for understanding the effect of heterogeneity
246 on the fracture performance.

247 **2.4 Hydraulic Fracture Conductivity versus Effective Stress**

248 Conductivity of the fracture will be reduced during the life of the well because of increasing stress on
249 the propping agents. The effective stress on the propping agent is the difference between the in-situ
250 stress and the flowing pressure in the fracture. As the well is produced, the effective stress on the
251 propping agent will normally increase, because flowing bottomhole pressure will be decreasing.
252 Parvizi et al. (2015b) explained the workflow of integration of this mechanism into the dynamic model.
253 This effect is measured in the laboratory by measuring the fracture conductivity with increasing
254 effective stress on proppants and the conductivity versus effective stress is obtained (Figure 3-a). The
255 results are then translated into the dynamic model in the form of a fracture transmissibility multiplier
256 versus pressure table (Figure 3-b). Grid cells that represent the fracture in the model could then be
257 assigned the fracture transmissibility multiplier versus pressure table that was created as illustrated in
258 Figure 3.



259
260 Figure 3. Translating fracture conductivity versus proppant stress (a) into fracture transmissibility
261 multiplier versus pressure (b) (Parvizi, et al, 2015a).

262 An important step in this study is the integration of the results of net pressure analysis with the outcome
263 of the analysis performed in this section on the change of fracture conductivity with effective stress.
264 Such integration is seen as a challenge due to the fact that the nature and detail level of these parameters
265 and analyses are different and there has not been a practical technique to capture and successfully

266 combine all the information gained through the application of each method. The following section
267 presents the way in which this challenge is overcome.

268 **2.5 Integration of Net Pressure Match, Well Test Data, PLT Results and Connectivity Behaviour**

269 Generally, the process of hydraulic fracture description involves using fracture design software to
270 match the net-pressure and report the fracture geometry (height, and half-length) and attributes such
271 as conductivity for each fracture. Post-job well test (well test carried out after hydraulic fracturing and
272 cleaning up) is the main reference to show the performance of the well. The problem is that the
273 assumptions of fracture in well test interpretation are based on an average fracture attribute and
274 geometry. This makes the comparison very difficult.

275 In order to evaluate fracture performance, we define a measurable parameter named Surface
276 Conductivity (SC_f) for the hydraulic fractures. This parameter should be an indication of the expected
277 fracture performance; thus, SC_f is directly proportional to fracture conductivity and its dimensions.
278 Therefore;

$$279 \quad SC_f \propto K_f \cdot w$$

$$280 \quad SC_f \propto 2 \cdot X_f$$

$$281 \quad SC_f \propto h_f$$

282 Where $K_f \cdot w$ is conductivity of hydraulic fracture, x_f is hydraulic fracture half length, and h_f is hydraulic
283 fracture height. Then, SC_f can be defined as fracture surface multiplied by fracture conductivity
284 (Equation 1). The unit of SC_f would be $mD \cdot ft^3$, but for simplicity of the analysis, the values would be
285 presented in $10^6 mD \cdot ft^3$ since the typical values for such a parameter will be in the order of 10^6 to 10^9 .

$$286 \quad SC_f = 2x_f \times h_f \times K_f \cdot w \qquad \text{Equation 1.}$$

287 In order to generalise the concept of SC_f for the wells with more than one fracture, SC is defined for
288 such wells as the summation of all the SC_f values of the fractures in the well (Equation 2).

$$289 \quad SC = \sum_{i=1}^n 2x_f \times h_f \times K_f \cdot w \quad \text{Equation 2.}$$

290 Integrating all the hydraulic fracture properties into one single parameter is the key advantage of SC.
291 It can therefore, be calculated for well test analysis outcome as well as net pressure match; Equation 3
292 and Equation 4.

$$293 \quad SC_{WTA} = \sum_{i=1}^n 2x_f \times h_f \times K_f \cdot w \quad \text{Equation 3.}$$

$$294 \quad SC_{NPM} = \sum_{i=1}^m 2x_f \times h_f \times K_f \cdot w \quad \text{Equation 4.}$$

295 Where

296 WTA= Well test analysis (post-frac well test)

297 NPM= Net pressure match for the fracture job

298 n= Number of hydraulic fractures that are assumed for well test match

299 m= Number of hydraulic fractures that are designed in hydraulic fracture design software

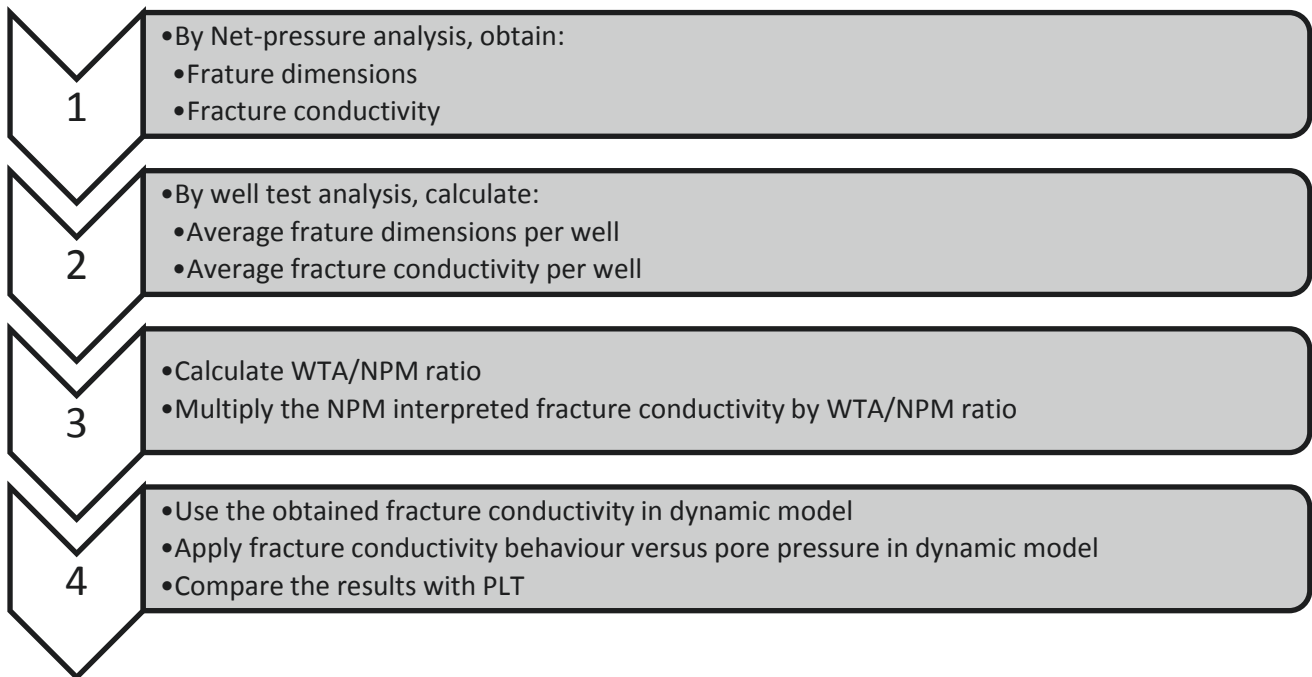
300 In order to integrate the results from the net pressure match and well test analysis, a new parameter is
301 proposed to be calculated: the WTA/NPM ratio (Equation 5). This ratio is the comparison of the
302 product of fracture surface area ($x_f \cdot h_f$) and fracture conductivity ($k_f \cdot w$) between the results derived
303 from well test analysis and net pressure matching. This ratio solves the issue of having different levels
304 of details for net-pressure-match versus well test analysis.

305 WTA/NPM ratio will be defined as:

$$306 \quad SC_{WTA}/SC_{NPM} = \left(\sum_{i=1}^n 2x_f \times h_f \times K_f \cdot w \right)_{WTA} / \left(\sum_{i=1}^m 2x_f \times h_f \times K_f \cdot w \right)_{NPM}$$

307 Equation 5.

308 This ratio is then used to adjust the fracture conductivity in the dynamic simulation model using the
309 proposed workflow shown in the Figure 4.



310

311 Figure 4. Workflow for integration of NPM, WTA, fracture conductivity behaviour and checking
312 against PLT data.

313 This technique has the following advantages:

- 314 1. It reduces the uncertainty of net pressure match output by a truth-checking scaling factor.
- 315 2. It makes history matching easier by improving initial guess accuracy.
- 316 3. It is able to correlate data from a source with fewer dimensions (well test analysis) to another
317 source with higher level of dimensions (conductivity distribution in fracture cells).
- 318 4. It gets the benefits of both techniques: details from net pressure match and validation from well
319 test and production data.
- 320 5. It captures the dynamics of connectivity and makes the forecasting more reliable.

321 This technique is validated by real field data and the results are discussed in the next section.

322 **3. Results and Discussion**

323 In this section, the application of the proposed technique on the field data is presented in a case study
 324 manner. First, as a diagnostic tool for fraced well performance, the WTA/NPM analysis is performed
 325 and cross checked with geological observations to support the conclusion. Then, production data (PLT)
 326 is shown to be in agreement with the findings of he WTA/NPM analysis. The impact of WTA/NPM
 327 ratio on reservoir dynamic modelling is discussed in details. Finally, the results of application of the
 328 proposed technique are validated using actual field data and evidences.

329 **3.1 WTA/NPM Analysis: A new proposed ratio for fraced well performance**

330 Well test interpretation has been carried out on each of the wells and the results in terms of fracture
 331 model (FC: finite conductivity), fracture conductivity (permeability x width), fracture half-length and
 332 fracture height are presented in the first section of Table 1. Interpretation of the net-pressure analysis
 333 per fracture (total of 24 fractures initiated) and the outcome in terms of fracture connectivity, fracture
 334 half-length and fracture height is reported in the last section of this table. Using Equation 5,
 335 SC_{WTA}/SC_{NPM} is calculated and stated in the column of WTA/NPM. WTA/NPM of 100% means the
 336 well behaves as it has been modelled. The range of WTA/NPM for this field varies from 35% to 174%
 337 which shows the wells which underperformed (Well B, D and E) or far outperformed (well A); Table
 338 1.

Well	Well test analysis per well					WTA/NPM	Net pressure match per fracture			
	Fracture Model	Kf.W (Frac) mD.ft	No. of Fractures	Fracture Half Length (ft)	Fracture Height (ft)		Average* Kf.W (Frac) mD.ft	Fracture Half Length (ft)	Fracture Height (ft)	Kf.W (Frac) mD.ft
A	FC	2500	4	300	250	174%	2039	220	230	1088
								200	220	3099
								200	120	1596
								250	180	1840
								200	240	2478
B	FC	1000	4	200	250	63%	1567	175	75	632
								210	250	403
								350	150	2169

								220	230	2106
								150	220	2008
C	FC	500	3	200	250	104%	802	200	60	195
								150	110	353
								252	198	1227
								320	160	463
								260	140	1102
D	FC	1220	3	202	150	35%	1279	420	150	2489
								350	180	1512
								580	115	601
								425	130	453
E	FC	2579	5	132	250	85%	2306	320	190	2043
								240	150	2075
								350	170	2216
								125	210	3251
								155	230	2442

339 Table 1. Results of WTA/NPM analysis of an actual field data in addition to calculated fracture
340 dimensions and conductivity by well test analysis and net pressure match.

341 The calculated WTA/NTM ratios lead to observations summarized in Table 2.

Well	WTA/NPM	Explanations
A	174%	Well productivity is exceptionally higher than the expected fracturing performance
B	63%	Well productivity is less than the expected fracturing performance
C	104%	NPM and WTA are in a good agreement i.e. the well productivity and interpreted fracture performances are similar.
D	35%	There is a problem in the well/reservoir that causes the well productivity to be so lower than the expected performance.
E	85%	Well productivity and interpreted fracture performance are similar.

342 Table 2 WTA/NPM analysis and explanations.

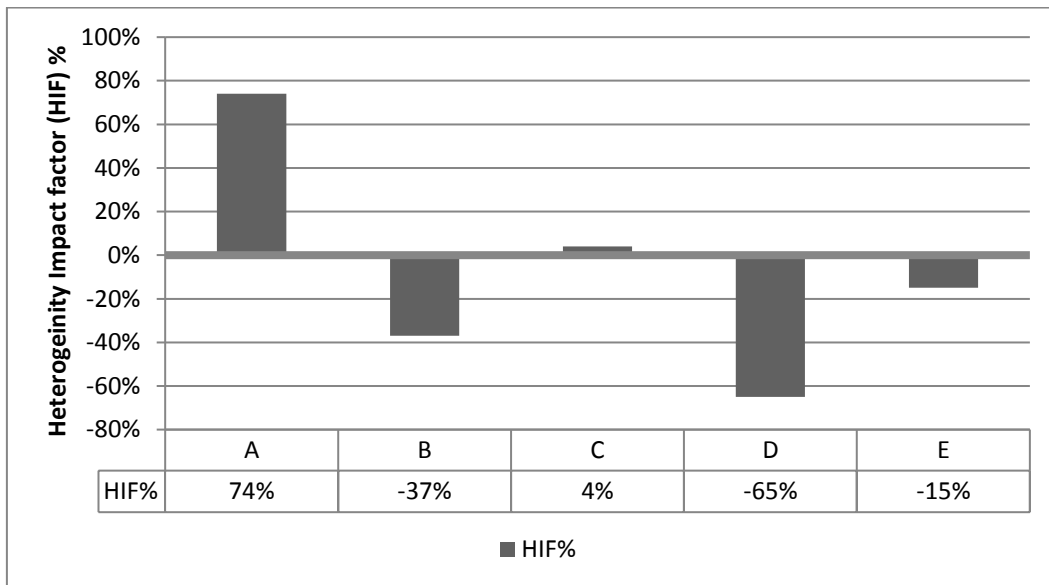
343 Using the calculated WTA/NPM, we introduce a new parameter called heterogeneity impact factor
344 (HIF) defined as below:

$$345 \text{HIF}\% = (\text{WTA/NPM} - 1)\% \quad \text{Equation 6.}$$

346 HIF quantifies the heterogeneity impact on hydraulic fracture performance because it is related to the
347 results of the observed data and considers the production period and the aerial extent of reservoir

348 properties in comparison to what has been expected by the performance of the fracing job. Generally,
 349 when the same fracture propagation is interpreted by different engineers/ researchers, different
 350 solutions in terms of fracture half length and height are obtained. The solutions with higher fracture
 351 half lengths usually have lower fracture height interpretations and vice versa. This gives rise to non-
 352 unique solutions for the same problem (Warpinski et al., 1994). HIF analysis, however, is basically
 353 using the multiplication of the fracture half length and fracture height, thus relaxing the solution against
 354 different interpretations. Furthermore, HIF analysis is, indeed, a repeatable workflow that can be run
 355 several times by adjusting the input parameters in their uncertainty range until the HIF uncertainty
 356 distribution is obtained based on which the rest calculations are performed.

357 Figure 5 shows the results of HIF% on the real field case. Well A far outperformed the expected
 358 hydraulic fracture performance whereas Well D dramatically underperformed. In the next section, we
 359 discuss the geological features to confirm the results.

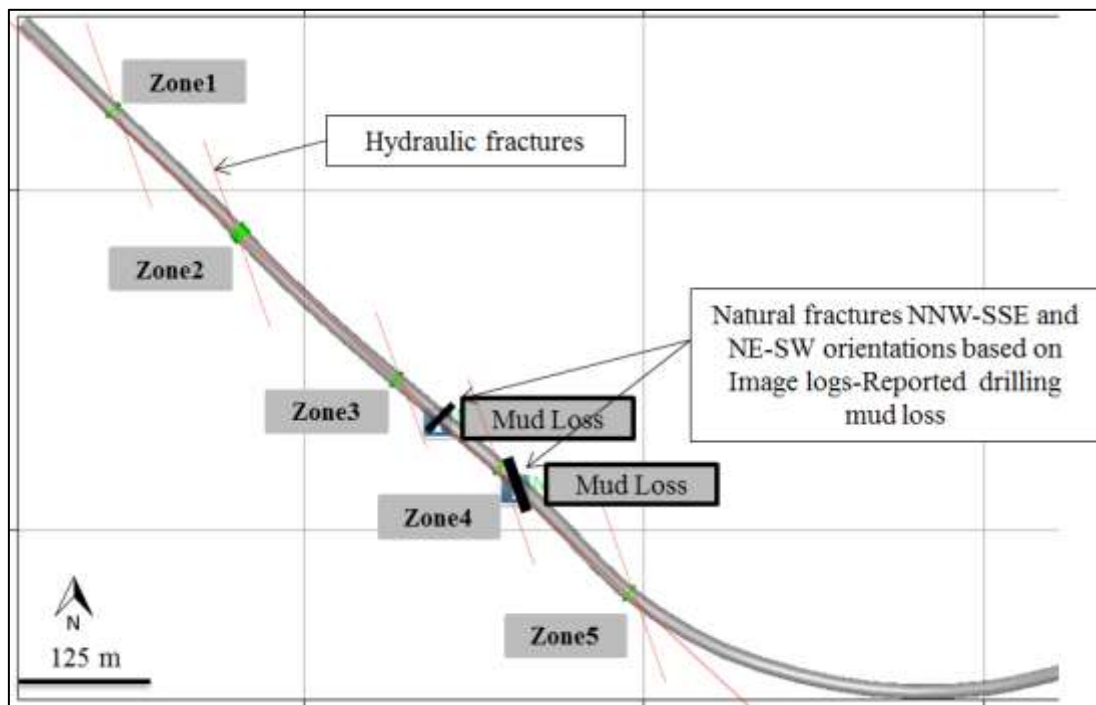


360
 361 Figure 5. Calculated heterogeneity impact factor per well.

362 **3.2 Geological Evidences Supporting the Results of WTA/NPA Analysis**

363 Well A has five fracturing zones in which zone 1 is the deepest and zone 5 is the shallowest, as
 364 exhibited in Figure 6. The final WTA/NPM ratio (SC_{WTA}/SC_{NPM}) for Well A is calculated to be 174%

365 which is much higher than the rest of the wells in this field. This means that there is remarkable
366 difference between the hydraulic fracture performance expectations (net pressure match) versus the
367 term WTA that is related to the production behaviour over a longer period. This is an indication of the
368 presence of an extra production mechanism that may be interpreted as natural fracture and/or more
369 permeable sands. This interpretation is confirmed by high mud-losses observed in the drilling report
370 and logging-while-drilling (LWD) image logs.

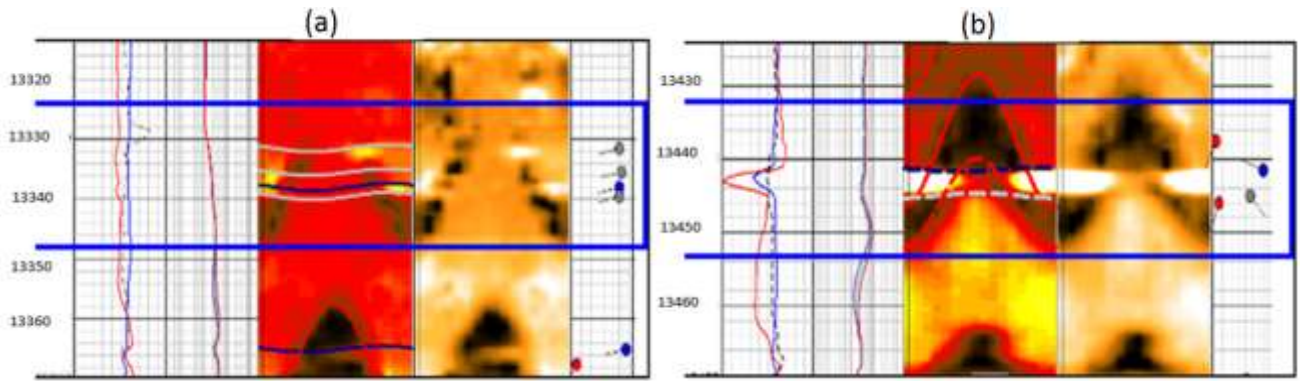


371

372

Figure 6. Well A trajectory, hydraulic fractures and mud loss positions.

373 Static losses of approximately 41bbl/hr were observed at 13,326ft MD and dynamic losses of
374 approximately 20bbl/hr were observed at 13,444ft MD. Based on the analysis of the density image
375 logs, it was found that the mud losses coincide with the presence of a cluster of low-density features
376 shown in Figure 7. The two features presented in the blue intervals of Figure 7 (a) and Figure 7 (b)
377 were interpreted as open fractures filled with drilling mud.



378

379 Figure 7. Density image logs show open fractures in the same regions where drilling mud losses
 380 happend while drilling Well A.

381 Aside from the two intervals where open fractures were interpreted, there was a substantial increase in
 382 the leakoff coefficient from the mini-frac ($0.0065 \text{ ft}/\sqrt{\text{min}}$) in zone 4 of Well A (perforation depth
 383 interval 13280-13290 ft MD); a mini-frac is performed without proppant and used as a diagnostic to
 384 aid with the final design of the main frac job. The main-frac (with proppant) of zone 4 had the highest
 385 leak off coefficient of $0.008 \text{ ft}/\sqrt{\text{min}}$. This further substantiated the existence of a higher permeable
 386 region that is connected to the hydraulic fracture. Figure 6 illustrates the trajectory, hydraulic fractures
 387 and reported mud-loss positions during drilling.

388 **3.3 Production Data and Application of Proposed Fracture Performance Ratio**

389 The PLT design was for two flowing passes, one at low rate the other at a high rate and one shut-in
 390 pass to evaluate the contribution of flow from each fracture. The tool was run in on wireline with the
 391 assistance of a tractor. Table 3 is a summary of the PLT results for Well A.

Zon e	Fracture half length (ft)	Fracture height (ft)	Fracture Kf.W (mD.ft)	SC (NPM) 10^6 mD.ft3	PLT flow contribution %
1	220	230	1088	110	24%
2	200	220	3099	273	14%
3	200	120	1596	77	4%
4	250	180	1840	166	22%

5	200	240	2478	238	36%
---	-----	-----	------	-----	-----

392 Table 3. PLT results summary for Well A compared with hydraulic fracture geometry from net
393 pressure match

394 A comparison of the SC vs PLT results is presented in Figure 8. The following observations have
395 been made:

396 **Zone 1:** The gas flow contribution is higher than the expected fracture performance. This can
397 be due to higher porosity at this region which needs seismic inversion techniques to be
398 confirmed. This will be investigated in next stage of this study.

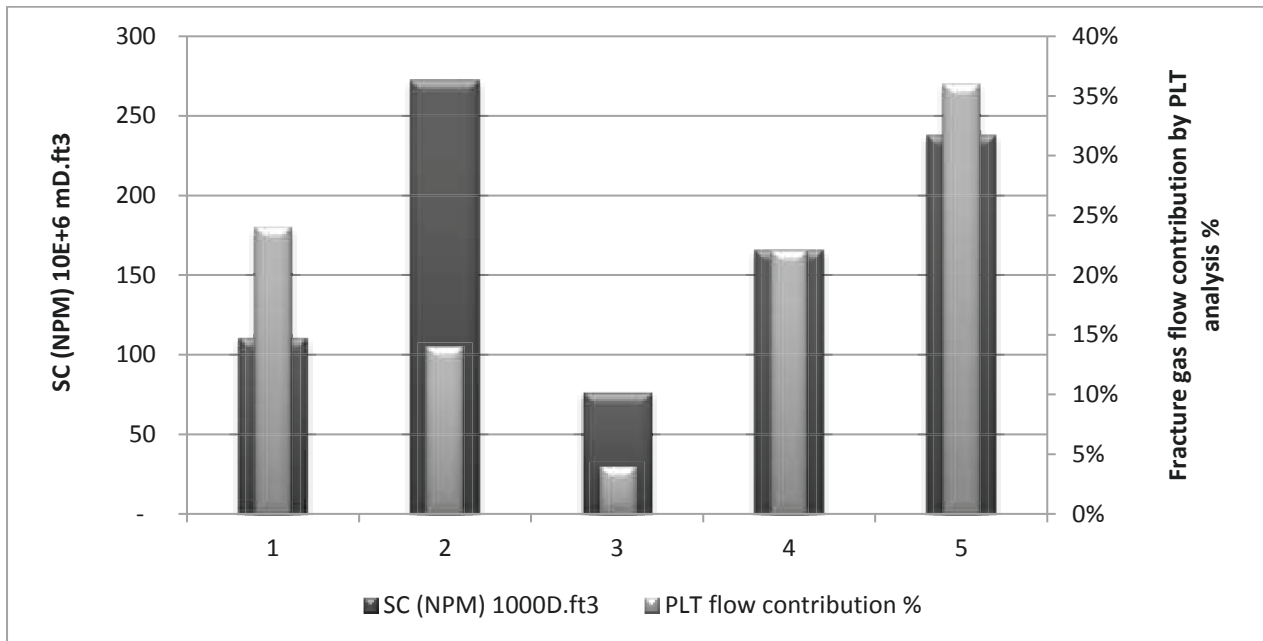
399 **Zone 2:** The gas flow contribution of this zone is consistent with SC(NPM) analysis. Low
400 fracture height caused the vertical confinement of hydraulic fracture.

401 **Zone 3:** The gas flow contribution of this zone is consistent with SC(NPM) analysis.

402 **Zone 4:** The gas flow contribution of this zone is higher than expected fracture performance
403 based on SC(NPM) analysis. This is linked to the high WTA/NPM ratio of well A.
404 Observations on image logs and drilling mud loss report on this zone confirmed open natural
405 fractures.

406 **Zone 5:** This zone is not connected to natural fractures by geological evidences but the
407 production logging results suggest the hydraulic fractures of this zone must be connected to
408 higher permeability conduits such as more permeable sands. In appraisal wells of this field, the
409 more permeable sands were observed in shallower geological layers than target layers for Well
410 A. The thickness, extension and permeability of these sands are a history matching parameters
411 for the dynamic model. Having defined all the properties and then applying the WTA/NPM
412 technique to longer the period of production, the history matching parameters are adjusted to
413 obtain a geologically valid thickness, lateral extension and possible permeability of these
414 conduits.

415 Based on such analysis, WTA/NPM ratio and production data are linked and aligned.



416

417 Figure 8. Comparison of SC (NPM) with PLT gas flow contribution

418

418 3.4 Impact of WTA/NPM ratio on Reservoir Dynamic Modelling

419

419 WTA/NPM technique identifies the wells which need to be tuned for having more reliable models.

420

420 The workflow of scaling the fracture cell properties is explained in Figure 4. The dynamic model is

421

421 created using LGR method to have more resolution around the wellbore. Having completed the

422

422 workflow (Figure 4), the dynamic model should be history matched using a reservoir simulator. The

423

423 reservoir simulator is run to compare the results of the input assumptions described in the above

424

424 sections with the real field data. Three years of gas production data and downhole gauge data was

425

425 available for this field.

426

426 The initial simulation run was close to the observed data. However, the observed data suggested more

427

427 pressure support from reservoir is required for the later production period. Well A water sample

428

428 analysis report also showed a small amount of formation water production which should also be

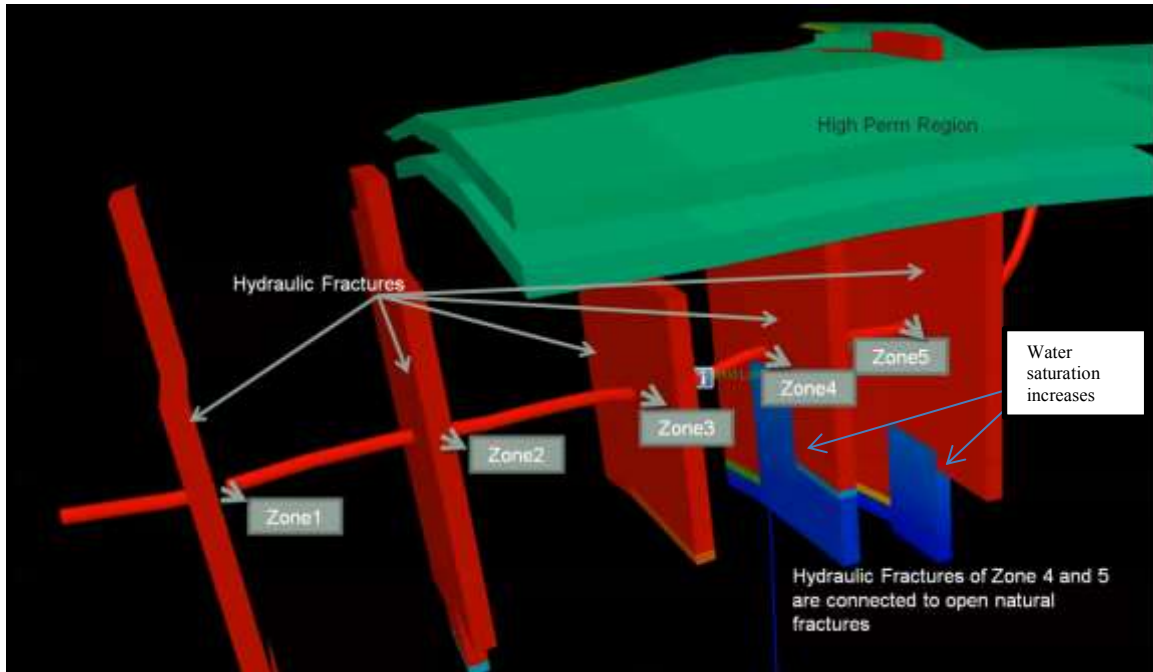
429

429 matched by the dynamic model.

430 In order to achieve a more representative dynamic model, the following history matching parameters
431 for Well A were considered:

- 432 • Extension of the more permeable region in the shallower layers as observed in the appraisal
433 well of the field
- 434 • Thickness of the more permeable region
- 435 • Connection of the more permeable region to the hydraulic fracture zones 4 and 5 to match
436 higher gas production contribution of these zones based on the observed PLT results
- 437 • Permeability (Y and Z direction) of global cells around the hydraulic fracture zone 4 to create
438 a higher perm connection to lower layers and also along the maximum horizontal stress. This
439 allows a flow path for water production by representation of vertical open natural fractures
440 which most likely are oriented in the maximum horizontal stress.

441 Using the above history matching parameters, the dynamic model was tuned and a match of gas
442 production rate, bottomhole pressure, production contribution of each zone and water production rate
443 was achieved. Figure 9 shows Well A along with five hydraulic fractures and water saturation increase
444 in Zone 4 due to its connection to natural fractures. The hydraulic fractures connect to an extensive
445 higher permeable region and natural fracture network, a 150mD high-permeability region is applied in
446 four sub-layers connected to zones 4 and 5 up to a distance of 200m around Well A. This area is
447 illustrated in Figure 9 (the cells with green colour).



448

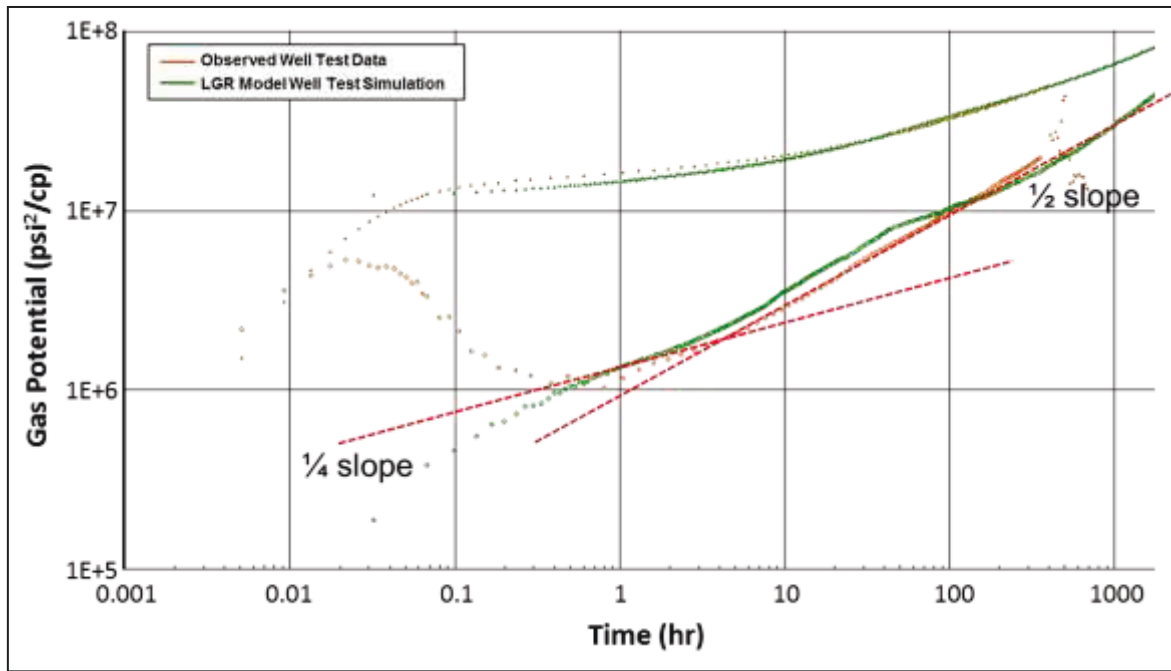
449

Figure 9. Water saturation on hydraulic fractures of Well A after history matching

450 **3.5 Validation of Proposed Technique using Actual Data**

451 In order to validate the dynamic model, pressure was predicted prior to the next summer shut down.
 452 Shut-in pressure data analysis is widely used in reservoir engineering to describe the production
 453 mechanism not only in the close proximity of the well but also in distances further away from the
 454 wellbore. The pressure difference and Bourdet derivative on a log-log plot is one of the key diagnostic
 455 plots in such an analysis. Matching these plots can demonstrate the accuracy of the model and it is
 456 ideal to validate the dynamic model. Therefore a simulation of shut-in build up data was performed
 457 during the summer shut down that lasted around three weeks (Figure 10). Comparing the simulation
 458 data to real observed data in Well A, a reasonable match was found, where the bilinear flow regime
 459 represent the finite conductivity fractures (1/4 slope), followed by a transition to a compound linear
 460 flow (1/2 slope).

461 The dynamic model is not supposed to match the early time data due to the effects of wellbore storage
462 however; it should match the pressure differences in the middle to late time regions and ideally the
463 Bourdet derivative. Figure 10 illustrates such a match, which is an evidence for validation of the model.



464

465 Figure 10. Pressure derivative of the LGR model prediction versus observed shut in data for Well A

4. Conclusions

- Different sources of information and analysis such as well test interpretation, net pressure study, fracture production data, fracture conductivity performance versus effective stress and reservoir dynamic modelling are discussed. The technical gap in data integration was identified and WTA/NPM technique is proposed as a solution.
- WTA/NPM technique integrates outcomes of well test interpretation and net pressure analysis in order to establish a quantitative diagnostic parameter for heterogeneity evaluation. This parameter is also used for scaling the NPM fracture conductivity to better represent the fractured well performance behaviour. The dynamic model initialised using such scaled fracture conductivity is more reliable.
- The heterogeneity impact factor (HIF) defined in this study represents a quantified value for expected performance of the hydraulic fracturing on each well. This quantified value represents the contribution of heterogeneity and creates a basis for comparing the wells of the same field with each other. It can also exhibit the impact of heterogeneity between different fields.
- Quantification of heterogeneity impact as a value is important as this value can be used for prediction of well production. This is by integrating tools of production simulation with HIF. HIF can also be used to filter the higher performance wells versus the other wells, purely due to heterogeneity of the area. This can help to analyse the patterns across different wells of the field for drilling targets of the next phases of field development.
- As the successful application of the proposed method has been confirmed by the geological and drilling evidences of encountering zones of natural fractures or high-permeability streaks, HIF analysis can prove valuable in gaining insight to the degree of such zonal heterogeneities which might be expected in other parts of the field in

case of the absence of enough geological or drilling information. In this sense, HIF analysis, once performed for enough number of wells in a field, could serve as powerful guide in better realising (or at least expecting) the reservoir heterogeneity by considering the HIF range of the wells in different locations of the field.

- HIF can also be used in uncertainty analysis of well production predictions as it gives a range of possible outcomes and, by linking to Decline curves analysis, it can generate hundreds of scenarios in few minutes. This is also another area of future work for the researchers.
- The proposed technique is applied on real field data and the results are presented which shows the robustness of the technique. As an evidence for the dynamic model validation, the prediction of the model is compared with a future 3-week shut-in pressure. The build-up pressure response and its derivative displayed an excellent match between the simulated and observed results.
- This study demonstrates a practical integrated approach towards modelling and evaluation of hydraulic fracture performance in heterogeneous reservoirs.

5. Nomenclature

C_{fD}	Dimensionless Fracture conductivity
DDA	Discontinuous Deformation Analysis
DEM	Distinct Element Model (DEM)
FC	Finite Conductivity
F_c	Fracture conductivity
HIF	Heterogeneity Impact Factor
k	Permeability
$K_{f.w}$	Connectivity of hydraulic fracture
LGR	Local grid refinement
LWD	logging-while-drilling
MD	Mesured depth
MMSFD	Million standard cubic feet
NPM	Net pressure match
PKN	Perkins-Kern-Nordgren theory

PLT	Production logging tool
P_n	Critical net pressure
PTA	Pressure transient analysis
S	Skin
SC_f	Surface Conductivity for a well with one hydraulic fracture
SC	Surface Conductivity for a well with multiple hydraulic fractures
w_f	Fracture width
WTA	Well test analysis
x_f	Fracture half-length

6. Acknowledgment

The authors would like to thank E.ON E&P UK, Dana Petroleum Plc and Bayerngas UK Ltd for providing the data and their permission to present and publish this material. Our appreciation goes to Wei-Cher Feng, Paul Arkley, Stephen Hart, Stewart Brotherton, Alex Kay, Aliona Kubyshkina, Azra Kovac, Helene Nicole, Terje Rudshaug, David Torr, Terry Wells, Mike Almeida, Paul Jeffs and Basil Al-Shamma for their useful insights and discussions.

References

1. Al-Zarouni, A. & Ghedan, S., 2012. Paving the Road for the First Hydraulic Fracturing in Tight Gas Reservoirs in Offshore Abu Dhabi. SPE152713.
2. Antoci, J. & Anaya, L., 2001. First Massive Hydraulic Fracturing Treatment in Argentina. SPE69581.
3. Bennett, C., Reynolds, A., Raghavan, R. & Elbel, J., 1986. Performance of Finite-Conductivity, Vertically Fractured Wells in Single-Layer Reservoirs. SPE11029.
4. Clarkson, C.R., 2013. Production data analysis of unconventional gas wells: Review of theory and best practices. *Int. J. of Coal Geology* 109–110, 101–146.
5. El-Ahmady, M. & Wattenbarger, R., 2004. Coarse Scale Simulation in Tight Gas Reservoirs. 2004-181 PETSOC.
6. Economides, M., Oligney, R. & Valko, P., 2002. *Unified Fracture Design*. Alvin(TX): Olsa Press.

7. Hamidi, F., Mortazavi, A., 2014. A new three-dimensional approach to numerically model hydraulic fracturing process. *Journal of Petroleum Science and Engineering*, Volume 124, Pages 451-467.
8. Hegre, T., 1996. *Hydraulically Fractured Horizontal Well Simulation*. SPE35506.
9. Huang, K., Ghassemi, A., 2012. Modeling 3D Hydraulic Fracture Propagation and Thermal Fracturing Using Virtual Multidimensional Internal Bonds, *Proceedings, Thirty-Sixth Workshop on Geothermal Reservoir Engineering Stanford University, Stanford, California, January 30 - February 2, 2012*.
10. Iwere, F., Moreno, J., Apaydin, O., Delaney, J., Thrush, P. & Gwaltney, J, 2004. Numerical Simulation of Thick, Tight Fluvial Sand. SPE90630.
11. Mirzaei-Paiaman A., The Severe Loss of Well Productivity in an Iranian Gas Condensate Carbonate Reservoir: Problem Identification and Remedy, *Energy Sources, Part A: Recovery, Utilization, and Environmental Effects*, Vol. 35, Issue 19.
12. Nadimi, S., Miscovic, I., McLennan J., 2016. A 3D peridynamic simulation of hydraulic fracture process in a heterogeneous medium. *Journal of Petroleum Science and Engineering*, Volume 145, Pages 444-452.
13. Nordgren, R.P., 1972. Propagation of a Vertical Hydraulic Fracture. SPE-3009-PA.
14. Parvizi, H., Rezaei-Gomari, S., Nabhani, F. & Feng, W., 2015a. Hydraulic Fracturing Performance Evaluation in Tight Sand Gas Reservoir with High Perm Streaks and Natural Fractures. SPE174338.
15. Parvizi, H., Rezaei-Gomari, S., Nabhani, F., Dastkhan, Z. & Turner, A., 2015b. A Practical Workflow for Offshore Hydraulic Fracturing Modelling: Focusing on Southern North Sea. SPE174339.
16. Perkins, T.K. and Kern, L.R., 1961. Widths of Hydraulic Fractures. *J. Pet. Tech.* 937-949; *Trans., AIME*, 222.
17. Shaoul, J., Ross, M., Spitzer, W., Wheaton, S., Mayland, P. & Singh, A., 2007. Massive Hydraulic Fracturing Unlocks Deep Tight Gas Reserves in India. SPE107337.
18. Schulte, W., 1986. Production From a Fractured Well With Well Inflow Limited to Part of the Fracture Height. SPE12882.

19. Sesetty V., Ghassemi, A., 2012. Modeling and analysis of stimulation for fracture network generation. In: PaperSGP-TR-194 presented at Thirty-Seventh Work-shop on Geothermal Reservoir Engineering Stanford University, Stanford, California, January30–February 1.
20. Sobhaniaragh, B., Mansur, W. J., Peters, F. C., 2016. Three-dimensional investigation of multiple stage hydraulic fracturing in unconventional reservoirs. *Journal of Petroleum Science and Engineering*, Volume 146, Pages 1063-1078.
21. Sousa, J. L., Carter, B. J., Ingraffea, A. R., 1993. Numerical simulation of 3D hydraulic fracture using Newtonian and power-law fluids. *International Journal of Rock Mechanics and Mining Sciences & Geomechanics Abstracts*, Volume 30, Issue 7, Pages 1265–1271.
22. Vos, B., Shaoul, J. & De Koning, K., 2009. Southern North Sea Tight-Gas Field Development Planning using Hydraulic Fracturing. SPE121680.
23. Wang, H. Y., 2015. Numerical modeling of non-planar hydraulic fracture propagation in brittle and ductile rocks using XFEM with cohesive zone method. *Journal of Petroleum Science and Engineering*, Volume 135, Pages 127-140.
24. Warpinski, N. R., Moschovidis, Z. A., Parker, C. D., Abou-Sayed, I. S. 1994. Comparison Study of Hydraulic Fracturing Models—Test Case: GRI Staged Field Experiment No. 3 (includes associated paper 28158). SPE-25890-PA. doi:10.2118/25890-PA.
25. Zhang, X., Jeffrey, R.G., Thiercelin, M., 2007. Deflection and propagation of fluid driven fractures at frictional bedding interfaces: A numerical investigation. *Journal of Structural Geology*, Volume 29, Issue 3, Pages 396–410.
26. Zhang, Z., Li, X., Yuan, W., He, J., Li, G., Wu, Y., 2015. Numerical Analysis on the Optimization of Hydraulic Fracture Networks, *Energies*, 8(10), 12061-12079; doi:10.3390/en81012061.
27. Zhang, Z., Peng, S., Ghassemi, A., Ge, X., 2016. Simulation of complex hydraulic fracture generation in reservoir stimulation. *Journal of Petroleum Science and Engineering*, Volume 146, Pages 272-285.
28. Zhao, X. & Young, R., 2009. Three-dimensional Dynamic Distinct Element Modelling Applied to Laboratory Simulation of Hydraulic Fracturing in Naturally Fractured Reservoirs. 2009-2697 SEG.

Appendix A

Fracture average width by net pressure match analysis (based on 24 hydraulic fracture jobs of a Southern North Sea field)

Well	Fracture width (in)	Well	Fracture width (in)	Well	Fracture width (in)	Well	Fracture width (in)	Well	Fracture width (in)
A	0.165	B	0.067	C	0.029	D	0.512	E	0.37
	0.371		0.053		0.036		0.188		0.247
	0.204		0.375		0.25		0.166		0.364
	0.318		0.298		0.104		0.106		0.208
	0.292		0.158		0.148		-		0.235